Pergamon

Tetrahedron 56 (2000) 2015–2023

TETRAHEDRON

Ruthenium Catalyzed One-pot Synthesis of Dihydro-pyrrol-2-one Derivatives from α,β-unsaturated Imines, Carbon Monoxide and Ethylene

Daniel Berger and Wolfgang Imhof*

Institut für Anorganische und Analytische Chemie der Friedrich-Schiller-Universität, August-Bebel-Strasse 2, D-07743 Jena, Germany

Received 13 January 2000; accepted 8 February 2000

Abstract—The use of $Ru_3(CO)_{12}$ as a precatalyst induces a catalytic C–C coupling reaction of α,β-unsaturated imines with CO to yield imines with an aldehyde function in β-position with respect to the C–N double bond. An intramolecular cyclization reaction takes place via the nucleophilic attack of the imine nitrogen towards the carbonyl carbon atom building up a pyrrol-2-one system. A second ruthenium catalyzed C–C coupling reaction leads to the formal insertion of one molecule of ethylene into a C–H bond of the pyrrol-2-one in *ortho* position with respect to the keto group. By this selective reaction cascade imines derived from cinnamaldehyde or crotonic aldehyde, respectively, produce 1,3-dihydro-pyrrol-2-one derivatives. The analogous reaction starting from β-naphthylaldimines yields 9b-ethyl-4-propionyl-2,9b-dihydro-benzo[*e*]isoindol-1-one derivatives as a new class of heterocyclic compounds.

Introduction

C–H activation reactions induced by transition metal compounds may well serve as models for the initial steps of catalytic C–C coupling reactions and thus have been intensively examined during the last years.[1] Previously we studied C–H activation reactions upon complexation of several types of aromatic imines with $Fe_2(CO)_9$.[2] The reactions proceed regioselectively via C–H bond cleavage in *ortho* position with respect to the imine substituent and subsequent intramolecular hydrogen migration reactions towards suitable acceptor sites in the ligand producing di- or trinuclear iron carbonyl complexes. In addition, acyclic α,β-unsaturated imines like cinnamaldehyde derivatives react with $Ru_3(CO)_{12}$ via reaction pathways also including C–H activation and subsequent hydrogen migration reactions to yield di-, tri- or tetranuclear ruthenium carbonyl complexes.[3] On the other hand, the same cinnamaldehyde derived ligands upon treatment with $Fe_2(CO)_9$ form (η^4-1-azadiene)$Fe(CO)_3$ complexes. In this reaction no C–H activation steps occur.[4]

It has also been shown previously that aromatic imines or ketones may be treated with CO and/or olefins in the presence of catalytic amounts of $Ru_3(CO)_{12}$ to yield the respective substitution products.[5] So an initial C–H activation reaction, which is closely related to the stoichiometric reactions mentioned above, and which is induced by some catalytically active ruthenium carbonyl species, allows the catalytic carbonylation or acylation of suitable aromatic starting compounds.

Herein we report the catalytic synthesis of pyrrol-2-one derivatives starting from α,β-unsaturated imines, CO and ethylene. The reaction is catalyzed by $Ru_3(CO)_{12}$ and the initial metal induced C–H activation/CO insertion reaction sequence triggers a highly selective reaction cascade leading to the observed heterocyclic compounds.

Results and Discussion

Catalytic reactions starting from acyclic α,β-unsaturated imines

We recently reported the catalytic synthesis of 1,3-dihydro-pyrrol-2-one derivatives obtained from the α,β-unsaturated acyclic imines **1a**–**f**, CO and ethylene[6] (Scheme 1).

It is obvious that the variation of the organic substituent at nitrogen (R′) determines the product distribution. If R′ is an electron withdrawing substituent, ethylene is inserted into the activated C–H bond leading to ethyl substituted imines as their *Z* and *E* isomers (**3a**, **3b**). The insertion of CO leads to the formation of the 1,3-dihydro-pyrrol-2-one derivatives **2a**–**f**. If the nucleophilicity of the azadiene π-system is increased by variation of R′ towards electron donating

Keywords: catalysis; pyrrolones; isoindoles; C–C bond formation; X-ray structural analysis.

* Corresponding author. Tel.: +49-3641-948128; fax: +49-3641-948102; e-mail: cwi@rz.uni-jena.de

0040–4020/00/$ - see front matter
PII: S0040-4020(00)00118-6

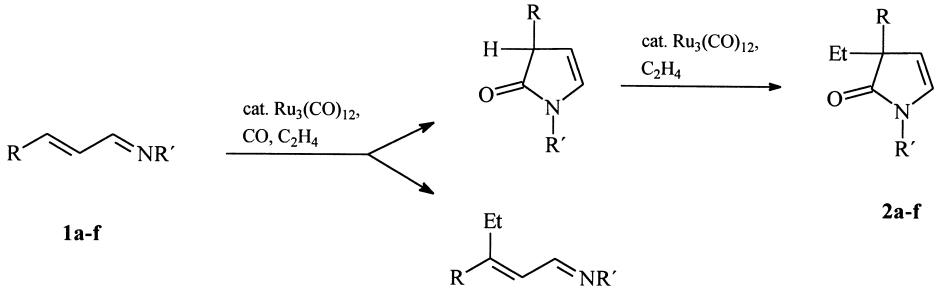

R	R′	compound	yield [%]	compound	yield [%]
Ph	4-CF_3-C_6H_4	**2a**	38	**3a**	58 (*Z*:*E*=1:2.5)
Ph	Ph	**2b**	49	**3b**	41 (*Z*:*E*=1:1)
Ph	4-Bu^t-C_6H_4	**2c**	15	-	
Ph	Bu^t	**2d**	44	-	
Ph	Cy	**2e**	93	-	
Me	Cy	**2f**	95	-	

Scheme 1.

substituents, CO is preferred for the first catalytic C–C coupling reaction and thus **2c–f** are formed selectively. In the case of **2c** and **2d** the yields are quite low, presumably because of the high steric demands of the *tert*-butyl groups. Using a cyclohexyl group as the organic substituent at nitrogen leads to an almost quantitative yield of **2e** or **2f**, respectively.

The formation of the pyrrole ring proceeds via a nucleophilic attack of the imine nitrogen towards the carbonyl carbon atom which was introduced into the molecule by the catalytic CO insertion reaction. Migration of the hydrogen atom from the aldehyde function towards C_3 of the pyrrole system leads to a 1,3-dihydro-pyrrol-2-one. The same compound has been proposed as an intermediate in a similar reaction reported by Murai, in which only CO was present in the reaction mixture.[7] It was pointed out that the 1,3-dihydro-pyrrol-2-one is the thermodynamically less stable compound and rearranges quantitatively to end up with the 1,5-dihydro-pyrrol-2-one derivative. We never observed the formation of 1,5-dihydro-pyrrol-2-ones, so the second catalytic C–C coupling reaction realized by the insertion of ethylene into the C–H bond in *ortho*-position with respect to the carbonyl moiety of the pyrrolone preserves the thermodynamically less favourable 1,3-dihydro-pyrrol-2-one system. In addition, the reaction we

Table 1. Turnover numbers (TON) and turnover frequencies (TOF) of the formation of **2e** depending on the catalyst/substrate ratio, temperature and reaction time

Cat:Substrate	*T* [°C]	*t* [h]	Conversion [%]	Selectivity of the formation of **2e**[a]	TON[b]	TOF [h^{-1}][b]
1:25	140	17	100	98	25 (8)	–
1:100	140	17	100	98	98 (33)	–
1:1000	150	138	100	84	840 (280)	–
1:5000	163	62	80	80	3200 (1067)	52 (17)
1:10000	140	67	88	70	3560 (1183)	53 (18)
1:15000	140	67	60	33	2970 (990)	44 (15)
1:50	150	1.5	13	98	10.8 (3.6)	7.2 (2.4)
1:100	150	1.5	22	98	12.7 (4.2)	8.5 (2.8)
1:500	150	5.33	18	98	88.2 (29.4)	16.5 (5.5)
1:1000	150	5.75	8.4	100	84 (28)	14.6 (4.9)

[a] Determined by integration of the ^1H NMR spectra of the crude reaction mixtures.
[b] Calculated per $Ru_3(CO)_{12}$, in brackets calculated per Ru, related on the formation of **2e**.

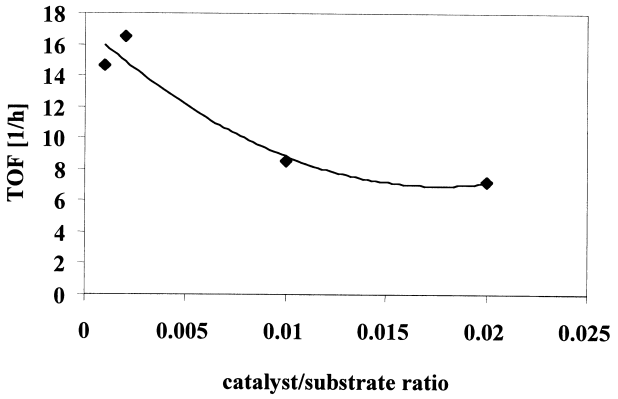

Figure 1. Dependency of the turnover frequency (TOF) of the formation of **2e** from the catalyst/substrate ratio.

describe herein leads to the formation of a new stereogenic center at C_3 of the pyrrole. In the future we will explore the possibility of achieving diastereoselective reactions by using chiral imines as the starting material or enantioselective reactions by using ruthenium catalysts with chiral ligands.

It has been pointed out in the literature that the dependency of the turnover frequency (TOF) of a catalytic reaction from the catalyst/substrate ratio is a way to distinguish between reactions in which a mononuclear organometallic species or a compound of higher nuclearity is the active catalyst.[8] If the catalytically active species is mononuclear the TOF is expected to increase if the concentration of the catalyst is decreased. However, if the TOF gets smaller by lowering the concentration of the catalyst an organometallic species of higher nuclearity is supposed to be the active catalyst.

The results concerning the percentage of conversion of the starting material as well as the selectivity of the formation of **2e** upon variation of the catalyst/substrate ratio, temperature and reaction time is shown in Table 1.

The experiments clearly demonstrate that for quite high catalyst/substrate ratios of 4 or 1 mol%, respectively, the reaction proceeds with quantitative conversion of the starting compound and high selectivity of the formation of **2e** within a short reaction time. If the catalyst/substrate ratio is lowered to 0.1 mol% the reaction time necessary to achieve a complete conversion of the starting compound increases dramatically. On the other hand, the selectivity of the formation of **2e** decreases due to decomposition of the product. If the catalyst/substrate ratio is further reduced to 0.01 mol% no complete conversion of the starting material may be achieved and the selectivity again is lower. Nevertheless, the turnover number (TON) clearly increases by reducing the catalyst/substrate ratio from 4 to 0.01 mol%. The maximum TON observed is about 3500 and thus much higher than those of realated reactions.[5,7] A catalyst/substrate ratio of 0.007 mol% obviously is too small since the percentage of conversion, the selectivity of the formation of **2e** as well as the TON and TOF decrease compared to the experiments with a higher concentration of the catalyst.

At the end of Table 1 four experiments are depicted in which the catalyst/substrate ratio was varied, but the reaction temperature was kept constant. All experiments were stopped after quite short reaction times in order to achieve a high selectivity of the formation of **2e** although the conversion of the starting material of course was quite low. Fig. 1 shows the dependency of the TOF from the catalyst/substrate ratio. It is obvious that the TOF increases as the concentration of the catalyst decreases. This may be indicative for a mononuclear ruthenium species as the active catalyst for this reaction. The fact that the TOF decreases slightly by changing the catalyst/substrate ratio from 0.2 to 0.1 mol% may be due to the short reaction time, since the induction period normally increases when the concentration of the catalyst is lowered.

2a–**f** as well as **3a** and **3b** were characterized by GC–MS, GC–IR and NMR measurements from the crude reaction mixtures. Crystals of **2f** suitable for X-ray structure determination were obtained by sublimation of the crude product. The compounds **2a**–**f** exhibit expected NMR spectroscopic properties. The most significant features in the ^{1}H NMR spectra are the two doublets representing the olefinic hydrogens at C_4 and C_5 of the pyrrole. They are observed in the range of δ=5.5–5.9 and δ=6.5–7.1, respectively. Another characteristic signal is the multiplet of the methylene group attached to the new stereogenic center at C_3 indicating the diastereotopicity of those hydrogen atoms. In addition, the methine proton of the cyclohexyl groups in **2e** and **2f** shows a considerable downfield shift to about δ=3.9, which by X-ray crystallography was shown to be

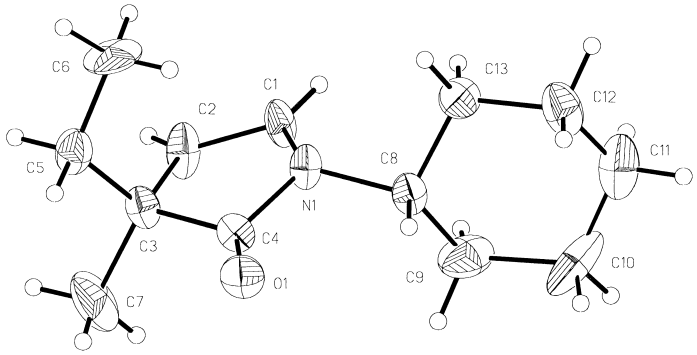

Figure 2. Molecular structure of *S*-**2f**. Selected bond lengths [pm] and angles [deg]: N1–C1 140(2), C1–C2 142(2), C2–C3 151(1), C3–C4 152.3(8), C4–O1 123.7(8), O1···H8 244(3); N1–C1–C2 106(2), C1–C2–C3 110.7(9), C2–C3–C4 101.2(5), C3–C4–N1 105.4(7), C4–N1–C1 113(1).

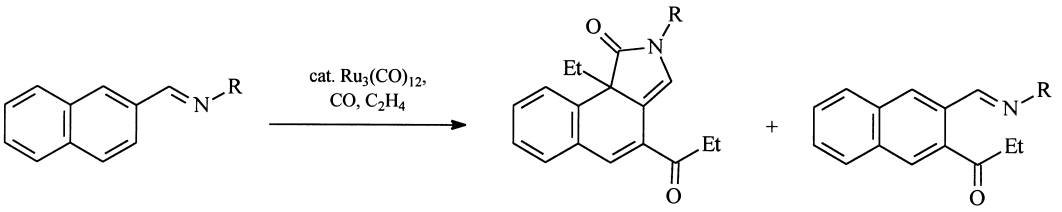

Scheme 2.

due to an intramolecular hydrogen bond between this proton and the carbonyl oxygen of the pyrrolone. This hydrogen bond obviously is also the reason for the observation of five different methylene carbon resonances in the ^{13}C NMR spectra of **2e** and **2f**.

The molecular structure of **2f** is shown in Fig. 2.[9] Since the synthesis of **2f** was carried out under achiral conditions the racemate of **2f** was produced. Fig. 1 shows the *S*-enantiomer, but both enantiomers are statistically disordered in the lattice. The bond lengths and angles show the expected values with the bonds at C3 showing values typical for carbon–carbon single bonds whereas the bond between C1 and C2 clearly is a double bond.

Catalytic reactions starting from β-naphthylaldimines

The reaction of imines derived from β-naphthylcarbaldehyde (**4a**, **4b**) with CO and ethylene catalyzed by $Ru_3(CO)_{12}$ is shown in Scheme 2.

The 9b-ethyl-4-propionyl-2,9b-dihydro-benzo[*e*]isoindol-1-one derivatives **5** always are the main products of this catalytic reaction and are formed in good to excellent yields; however, the 3-(propionyl)-napthyl-2-carbaldimines **6**, in which only one C–H function of the starting compound has been activated, is formed as a major side product. This is in contradiction to a report in the literature where under nearly identical reaction conditions a derivative of **6** was described as the only product of the reaction.[5b] In addition, we found product **6** to be fairly unstable on silica gel or GC columns which were used in attempted separations and thus no elemental analysis of pure **6** could be carried out so far. Both **6a** and **6b** were identified by their NMR signals in the crude reaction mixtures and by GC–MS.

The formation of compounds of type **5** requires a selective reaction cascade including the insertion of two molecules of CO and two molecules of ethylene as well as an intramolecular cyclization reaction. The absence of derivatives of **5** without an additional propionyl group could be explained by a high reactivity of these, which makes them a preferable substrate to enter a second reaction cycle yielding the observed main product **5**. Or the catalytic reaction leading to **5** works with **6** as the starting material only, meaning that **6** is an intermediate in the reaction to **5**. This assumption is supported by two facts. First the complexation of β-naphthylaldimines with $Fe_2(CO)_9$ leads to the activation of C–H bonds in 3-position of the naphthalene core exclusively. A preference of this position compared to the other *ortho*-position would also be expected for a catalytic C–H activation induced by $Ru_3(CO)_{12}$ since it is well known that those reactions are thermodynamically controlled.[1] Thus the formation of an isomer of **6** with the propionyl group in 1-position of the naphthalene seems to be unlikely. And second, the presumption of **6** being an intermediate in the formation of **5** is supported by the time dependency of the product distribution of the reaction. Fig. 3 shows the percentage of conversion of the starting material as well as the yield of **5b** and **6b**, respectively.

Fig. 3 shows that the concentration of **6b** increases quite

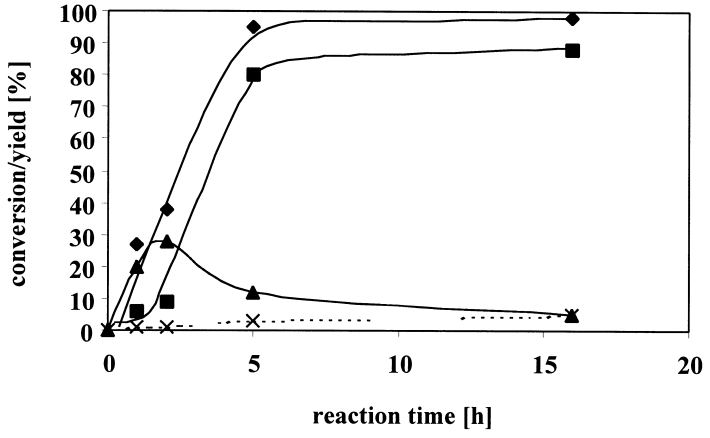

Figure 3. Time dependency of the percentage of conversion of the starting compound as well as the yields of the products ▲=yield **6b**, ■=yield **5b**, ×=yield by-products, ◆=percentage of conversion.

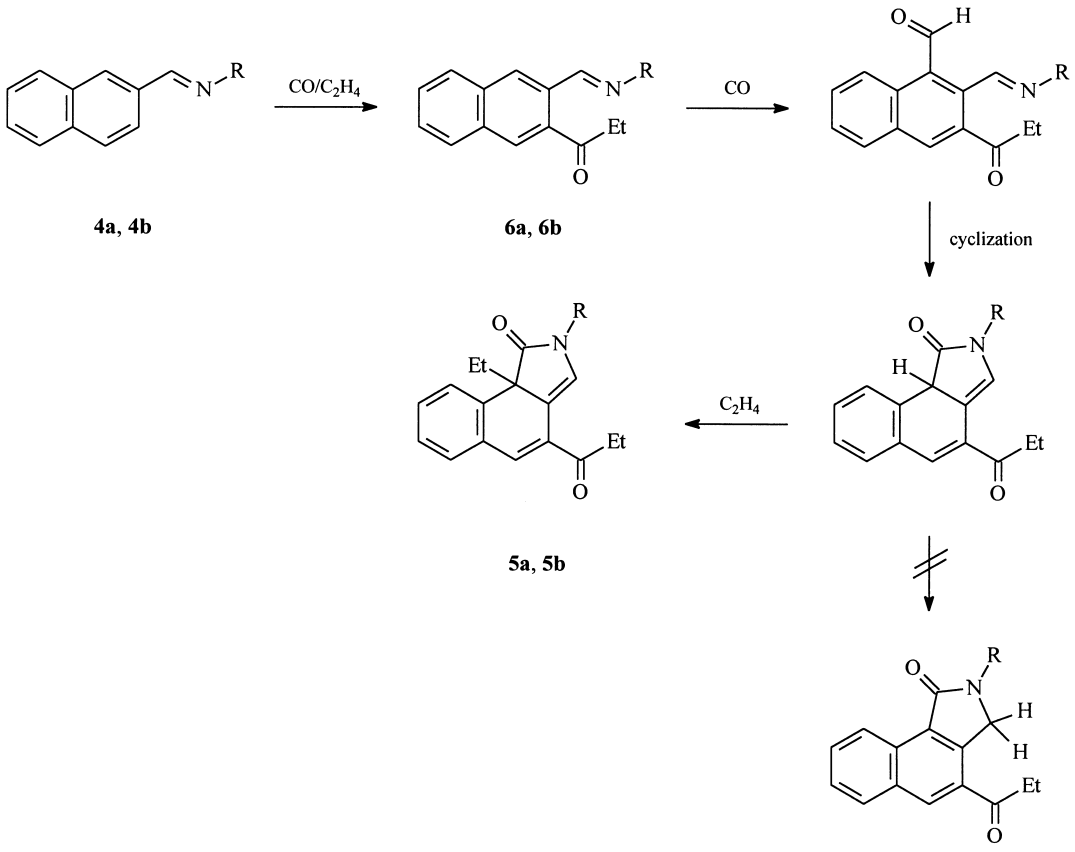

Scheme 3.

rapidly to reach a maximum after about 2 h. Afterwards the ratio of **6b** compared to the other products of the reaction decreases. The formation of **5b** starts after an induction period of about 1.5 h to reach about 80% after 5 h. The concentration of by-products that were not identified reaches about 6% after 16 h. The percentage of conversion of the starting material already is 95% after 5 h and comes up to nearly 100% in the next 11 h. If the reaction leading to the formation of **5a** and **6a**, respectively, is monitored, a quite similar picture is obtained. The most significant difference is the fact that the reaction proceeds much more slowly, perhaps due to the lower nucleophilicity of the imine nitrogen caused by the phenyl substituent compared to the cyclohexyl group. The maximum of **6a** is reached after a reaction time of 18 h and also starts to decrease afterwards. The formation of **5a** also starts after an induction period, but in this reaction the concentration of **5a** reaches a maximum after 60 h and then also begins to decrease, whereas the ratio of by-products that we were not able to identify increases.

In Scheme 3 a possible reaction cascade leading to **5** is shown. After a first insertion of CO and ethylene into the activated *ortho* C–H bond, **6** is produced in analogy to reported reactions, where acylations in *ortho*-positions of several aromatic ketones and imines were reported.[5] Starting with the second CO insertion the reaction follows the same pathway as it was explained for the formation of 1,3-dihydro-pyrrol-2-one derivatives. The five membered heterocyclic ring is closed by an intramolecular cyclization including a 1,2-H migration towards the former 1-position of the naphthalene which therefore becomes a new stereogenic center. The new C–H bond in a final step is activated again, followed by a second ethylene insertion to yield the observed main product **5**. As it was observed in the reaction of cinnamaldehyde or crotonic aldehyde derivatives the second ethylene insertion is also faster than a rearrangement process which normally would have been expected to occur after the cyclization reaction to yield the isomeric 4-propionyl-2,3-dihydro-benzo[*e*]isoindol-1-ones. Although we cannot completely rule out other possible reaction sequences, this is the most likely one, since it explains the time dependency of the **5**:**6** ratio and is also in agreement with all the data on similar reactions reported in the literature.

Both **5a** and **5b** are characterized by NMR, IR and MS spectroscopy as well as elemental analysis and X-ray crystallography.[10] In the ^{1}H NMR spectra of **5a** and **5b** the methylene hydrogens of the ethyl group next to the stereogenic center again are diastereotopic and thus show a characteristic coupling pattern. The resonance of the methylene protons corresponding to the exocyclic propionyl substituent is observed as the expected quartet. In analogy to the spectra of **2e** and **2f** the signal of the methine hydrogen atom in the cyclohexyl ring of **5b** shows a considerable downfield shift to δ=3.97 indicating a fairly strong intramolecular interaction with the adjacent carbonyl oxygen. The short intramolecular H–O distance of 252 pm found in the crystal structure of **5b** complies with this and lies in the range of quite strong hydrogen bonding.[12] The NMR spectra of the crude reaction mixtures show signals typical

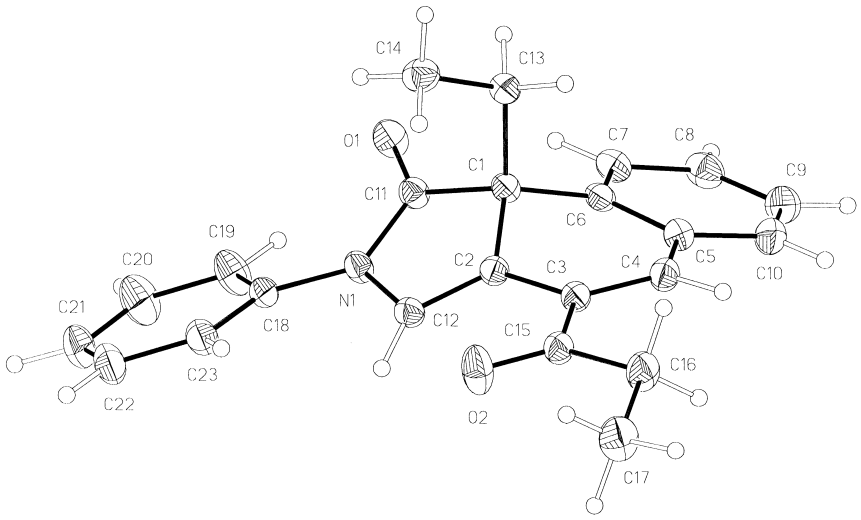

Figure 4. Molecular structure of **5a** (the numbering scheme has been adopted for **5b**). Selected bond distances [pm] and angles [deg]: **5a**: C1–C2 151.0(2), C1–C11 153.8(2), C11–N1 139.4(2), C2–C12 133.7(2), C12–N1 142.7(2), C1–C6 152.4(2), C2–C3 146.0(2), C6–C1–C2 109.8(1), C6–C1–C11 116.5(1), C6–C1–C13 108.4(1), C2–C1–C11 102.7(1), C2–C1–C13 112.3(1), C11–C1–C13 107.2(1), C4–C3–C2 116.9(2), C3–C2–C12 132.3(2), C2–C12–N1 111.3(2), C12–N1–C11 109.5(1), N1–C11–C1 107.0(1); **5b**: C1–C2 152.0(5), C1–C11 154.4(5), C11–N1 137.6(5), C2–C12 134.1(5), C12–N1 142.4(4), C1–C6 150.3(5), C2–C3 145.6(4), C6–C1–C2 110.7(3), C6–C1–C11 118.2(3), C6–C1–C13 107.6(3), C2–C1–C11 102.4(3), C2–C1–C13 110.9(3), C11–C1–C13 106.9(3), C4–C3–C2 117.3(3), C3–C2–C12 131.8(3), C2–C12–N1 110.9(3), C12–N1–C11 110.6(3), N1–C11–C1 106.8(3).

for the propionyl groups of **6a** and **6b**. Together with the results of GC–MS measurements this led us to the conclusion that **6a** and **6b** were formed as side products of the catalysis.

The bond distances and angles determined by X-ray structure analysis clearly reflect the description of **5a** and **5b** as dihydro-benzo[*e*]isoindol-1-one derivatives (Fig. 4). The carbon atom in 1-position of the former naphthalene core is tetrahedrally surrounded with the four C–C bonds showing values typically found for single bonds. On the other hand, the C–C bond of C_2 of the former naphthalene system with the former imine carbon atom shows a bond length of 134.5(5) pm clearly indicating a double bond. The other bond lengths and angles show expected values.

In conclusion, there are two possible pathways in ruthenium catalyzed C–C bond forming reactions. One is an intramolecular cyclization reaction following the first C–C coupling with CO yielding a dihydro-pyrrol-2-one system or a dihydro-benzo[*e*]isoindol-1-one derivative depending on the starting compound. One molecule of ethylene is then inserted into the C–H bond of the heterocyle in *ortho* position to the carbonyl function.

The second is a subsequent insertion of CO and C_2H_4 to produce propionyl moieties in *ortho* position to the imine function of aromatic imines. Starting from β-naphthylaldimines, both possibilities are realized on a single substrate molecule in a multistep one-pot reaction with both good selectivity and yield.

Since compounds containing a γ-lactam subunit are very interesting molecules with respect to pharmaceutical purposes,[11] the availability of these 1,3-dihydro-pyrrol-2-one as well as the 2,9b-dihydro-benzo[*e*]isoindol-1-one derivatives may well be a useful synthetic strategy towards new active substances.

Experimental

General

All procedures were carried out in anhydrous toluene as purchased from Aldrich. $Ru_3(CO)_{12}$ was purchased from Strem Chemicals and used without further purification. GC were done using a Chrompack CP 9000, carrying gas He; GC–MS spectra were carried out on a Finnigan MAT SSQ 710 instrument; GC–IR spectra on a Perkin–Elmer FT-IR System 2000; NMR spectra were recorded on a Bruker DRX 400 spectrometer (^{1}H, 400 MHz; ^{13}C, 100.6 MHz; $CDCl_3$ as internal standard); structure determinations of **2f**, **5a** and **5b** were carried out on an Enraf Nonius Kappa CCD diffractometer, crystal detector distance 25 mm, 180 frames, using graphite monochromated Mo-K_α radiation. The crystals were mounted in a stream of cold nitrogen. Data were corrected for Lorentz and polarisation effects but not for absorption. The structures were solved using direct methods and refined by full-matrix least squares techniques against F^2.[12] Computations were done with the program XPMA and the molecular structure was drawn using the program XP.[13,14] Additional material on the structure analysis is available from the Cambridge Crystallographic Data Centre by mentioning the deposition number 182/1302 (**2f**), 138815 (**5a**) and 138814 (**5b**).

Preparation of the compounds

In a typical experiment a total of 1 mmol of the corresponding imine (**1a**: 275 mg, **1b**: 207 mg, **1c**: 263 mg, **1d**: 187 mg, **1e**: 213 mg, **1f**: 151 mg, **4a**: 231 mg, **4b**: 237 mg), together with 4 mol% $Ru_3(CO)_{12}$ (25 mg), was put into a 100 ml stainless steel autoclave together with 3 ml of toluene. The autoclave was pressurized with 12 atm of CO and 8 atm of C_2H_4. The reaction temperatures and the reaction times used may be seen in Table 1 and Fig. 3. After the system was cooled down the CO and C_2H_4 was

released and the resulting brown-red solution was transferred to 25 ml Schlenk tube. The solvent was evaporated in vacuo which gave a brown oil for the reactions starting from **1a**–**f**. This oily residue was used for the GC-, GC–MS-, GC–IR- and NMR-measurements. In addition, colourless crystals of **2f** were obtained by sublimation from the crude brown oil at 10^{-2} Torr and 40°C. In the synthesis of **5a** and **5b** the products precipitated if the yield exceeded 70%. Recrystallization from toluene gave pale yellow fluorescenting crystals of **5a** or **5b**. In reactions without precipitation of **5**, separation can be achieved by preparative TLC on silica gel plates with toluene as eluent.

***N*-(4′trifluormethyl-phenyl)-3-ethyl-3-phenyl-1,3-dihydro-pyrrol-2-one 2a.** MS (EI): *m/z* (%) 331 (M^+, 61), 316 ($C_{18}H_{13}F_3NO^+$, 2), 312 ($C_{19}H_{16}F_2NO^+$, 4), 302 ($C_{18}H_{11}F_3NO^+$, 100), 287 ($C_{16}H_8F_3NO^+$, 5), 274 ($C_{15}H_7F_3NO^+$, 11), 204 ($C_{14}H_6NO^+$, 2), 172 ($C_{11}H_{10}NO^+$, 28), 145 ($C_{10}H_9O^+$, 24), 128 ($C_{10}H_8^+$, 7), 115 ($C_9H_7^+$, 7), 103 ($C_8H_7^+$, 5), 91 ($C_7H_8^+$, 4), 77 ($C_6H_5^+$, 3), 51 ($C_4H_3^+$, 2); ^{1}H NMR ($CDCl_3$, 298 K) [ppm]: 0.91 (t, $^3J_{HH}$=7.1 Hz, 3H, CH_3), 2.10–2.21 (m, 2H, CH_2), 5.91 (d, $^3J_{HH}$=4.8 Hz, 1H,=CH), 7.08 (d, $^3J_{HH}$=4.8 Hz, 1H,=CH), 7.12–7.65 (m, 9H, $C_{ar}H$); IR (GC-IR) [cm^{-1}]: 3071 w, 2976 w, 2936 w, 1748 m, 1611 m, 1521 w, 1383 m, 1324 vs, 1173 m, 1145 s, 1068 m, 872 w, 840 w, 696 w.

***N*-(4′-trifluormethyl-phenyl)-3-phenyl-pent-2-enyliden-amine 3a.** MS (EI): *m/z* (%) 302 (M^+−H, 100), 287 ($C_{17}H_{13}F_3N^+$, 9), 274 ($C_{16}H_{12}F_3N^+$, 13), 217 ($C_{16}H_{12}N^+$, 2), 198 ($C_{10}H_7F_3N^+$, 2), 172 ($C_8H_5F_3N^+$, 5), 158 ($C_{11}H_{12}N^+$, 4), 143 ($C_{10}H_9N^+$, 24), 128 ($C_{10}H_8^+$, 20), 115 ($C_9H_7^+$, 16), 91 ($C_7H_7^+$, 8), 77 ($C_6H_5^+$, 4), 51 ($C_4H_3^+$, 3); ^{1}H NMR (Z-isomer, $CDCl_3$, 298 K) [ppm]: 1.14 (t, $^3J_{HH}$=7.5 Hz, 3H, CH_3), 2.93 (q, $^3J_{HH}$=7.5 Hz, 2H, CH_2), 6.77 (d, $^3J_{HH}$=9.6 Hz, 1H,=CH), 7.05–7.45 (m, 9H, $C_{ar}H$), 8.55 (d, $^3J_{HH}$=9.6 Hz, 1H, N=CH); ^{1}H NMR (E-isomer, $CDCl_3$, 298 K) [ppm]: 1.11 (t, $^3J_{HH}$=7.4 Hz, 3H, CH_3), 2.63 (q, $^3J_{HH}$=7.4 Hz, 2H, CH_2), 6.52 (d, $^3J_{HH}$=9.6 Hz, 1H,=CH), 7.05–7.45 (m, 9H, $C_{ar}H$), 8.01 (d, $^3J_{HH}$=9.6 Hz, 1H, N=CH); IR (GC-IR, Z-isomer) [cm^{-1}]: 3075 w, 2954 w, 1617 s, 1527 m, 1324 vs, 1267 m, 1188 m, 1167 m, 1132 s, 1069 m, 836 w; IR (GC-IR, E-isomer) [cm^{-1}]: 3072 w, 3035 w, 2943 w, 1610 m, 1525 w, 1325 vs, 1264 w, 1168 m, 1134 s, 1069 m, 832 w, 744 w, 723 w.

***N*-phenyl-3-ethyl-3-phenyl-1,3-dihydro-pyrrol-2-one 2b.** MS (EI): *m/z* (%) 263 (M^+, 62), 248 ($C_{17}H_{14}NO^+$, 2), 234 ($C_{16}H_{12}NO^+$, 100), 219 ($C_{16}H_{11}O^+$, 3), 206 ($C_{15}H_9O^+$, 7), 178 $C_{13}H_5O^+$, 1), 144 ($C_{10}H_8O^+$, 3), 128 ($C_{10}H_8^+$, 5), 115 ($C_9H_7^+$, 6), 104 ($C_8H_8^+$, 27), 91 ($C_7H_7^+$, 3), 77 ($C_6H_5^+$, 20), 51 ($C_4H_3^+$, 4); ^{1}H NMR ($CDCl_3$, 298 K) [ppm]: 0.84 (t, $^3J_{HH}$=7.4 Hz, 3H, CH_3), 2.02–2.13 (m, 2H, CH_2), 5.78 (d, $^3J_{HH}$=5.2 Hz, 1H,=CH), 6.97 (d, $^3J_{HH}$=5.2 Hz, 1H,=CH), 7.08–7.51 (m, 10H, $C_{ar}H$); IR (GC-IR) [cm^{-1}]: 3072 m, 3047 w, 2976 m, 2933 w, 2889 w, 1745 s, 1598 s, 1501 vs, 1383 vs, 1326 m, 1301 m, 1203 s, 1095 w, 869 w, 760 w, 692 s.

***N*-phenyl-3-phenyl-pent-2-enyliden-amine 3b.** MS (EI): *m/z* (%) 234 (M^+−H, 100), 219 ($C_{16}H_{13}N^+$, 8), 206 ($C_{15}H_{11}N^+$, 23), 178 ($C_{13}H_7N^+$, 1), 158 ($C_{11}H_{12}N^+$, 2), 143 ($C_{10}H_9N^+$, 7), 128 ($C_{10}H_8^+$, 9), 115 ($C_9H_7^+$, 8), 104 ($C_8H_8^+$, 6), 91 ($C_7H_7^+$, 4), 77 ($C_6H_5^+$, 16), 51 ($C_4H_3^+$, 6); ^{1}H NMR (Z-isomer, $CDCl_3$, 298 K) [ppm]: 1.11 (t, $^3J_{HH}$=7.6 Hz, 3H, CH_3), 2.87 (q, $^3J_{HH}$=7.6 Hz, 2H, CH_2), 6.66 (d, $^3J_{HH}$=9.5 Hz, 1H,=CH), 7.12–7.47 (m, 10H, $C_{ar}H$), 8.53 (d, $^3J_{HH}$=9.5 Hz, 1H, N=CH); ^{1}H NMR (E-isomer, $CDCl_3$, 298 K) [ppm]: 1.07 (t, $^3J_{HH}$=7.6 Hz, 3H, CH_3), 2.59 (q, $^3J_{HH}$=7.6 Hz, 2H, CH_2), 6.45 (d, $^3J_{HH}$=9.6 Hz, 1H,=CH), 7.12–7.47 (m, 10H, $C_{ar}H$), 7.98 (d, $^3J_{HH}$=9.6 Hz, 1H, N=CH); IR (GC-IR, Z-isomer) [cm^{-1}]: 3070 s, 3034 m, 2980 m, 2942 w, 2886 w, 1636 s, 1599 vs, 1503 s, 1302 m, 1162 w, 759 m, 697 m; IR (GC-IR, E-isomer) [cm^{-1}]: 3071 s, 3034 m, 2976 s, 2945 m, 2890 w, 1631 s, 1598 vs, 1502 s, 1308 w, 1251 w, 1211 w, 761 m, 699 s.

***N*-(4′-*tert*-butyl-phenyl)-3-ethyl-3-phenyl-1,3-dihydro-pyrrol-2-one 2c.** MS (EI): *m/z* (%) 319 (M^+, 79), 304 ($C_{21}H_{22}NO^+$, 29), 290 ($C_{20}H_{20}NO^+$, 100), 276 ($C_{19}H_{18}NO^+$, 8), 234 ($C_{17}H_{14}O^+$, 5), 206 ($C_{15}H_{10}O^+$, 2), 160 ($C_{11}H_{12}O^+$, 10), 128 ($C_{10}H_8^+$, 8), 115 ($C_9H_7^+$, 7), 91 ($C_7H_7^+$, 8), 77 ($C_6H_5^+$, 3), 57 ($C_4H_9^+$, 3); ^{1}H NMR ($CDCl_3$, 298 K) [ppm]: 0.88 (t, $^3J_{HH}$=7.4 Hz, 3H, CH_3), 1.30 (s, 9H, CH_3), 2.08–2.14 (m, 2H, CH_2), 5.79 (d, $^3J_{HH}$=5.2 Hz, 1H,=CH), 6.99 (d, $^3J_{HH}$=5.2 Hz, 1H,=CH), 7.11–7.54 (m, 9H, $C_{ar}H$); IR (GC-IR) [cm^{-1}]: 3070 w, 2971 vs, 2887 w, 1734 s, 1610 m, 1518 vs, 1384 vs, 1327 m, 1301 m, 1265 w, 1203 m, 1087 w, 875 m, 833 w, 761 w, 728 w, 695 m.

***N*-(*tert*-butyl)-3-ethyl-3-phenyl-1,3-dihydro-pyrrol-2-one 2d.** MS (EI): *m/z* (%) 243 (M^+, 38), 228 ($C_{15}H_{18}NO^+$, 3), 214 ($C_{14}H_{16}NO^+$, 5), 200 ($C_{13}H_{14}NO^+$, 3), 187 ($C_{12}H_{13}NO^+$, 52), 172 ($C_{11}H_{10}NO^+$, 34), 158 ($C_{10}H_8NO^+$, 100), 144 ($C_{10}H_8O^+$, 10), 128 ($C_{10}H_8^+$, 11), 115 ($C_9H_7^+$, 18), 103 ($C_8H_7^+$, 16), 91 ($C_7H_7^+$, 4), 77 ($C_6H_5^+$, 5), 57 ($C_4H_9^+$, 16), 41 ($C_3H_5^+$, 11); ^{1}H NMR ($CDCl_3$, 298 K) [ppm]: 0.80 (t, $^3J_{HH}$=7.3 Hz, 3H, CH_3), 1.43 (s, 9H, CH_3), 1.90–2.05 (m, 2H, CH_2), 5.51 (d, $^3J_{HH}$=5.1 Hz, 1H,=CH), 6.75 (d, $^3J_{HH}$=5.1 Hz, 1H,=CH), 7.24–7.55 (m, 5H, $C_{ar}h$); IR (GC-IR) [cm^{-1}]: 3069 w, 2978 s, 2933 m, 2888 w, 1720 vs, 1608 w, 1494 w, 1464 w, 1374 m, 1275 m, 1243 s, 1177 w, 1031 w, 896 w, 804 w, 758 w, 692 m.

***N*-cyclohexyl-3-ethyl-3-phenyl-1,3-dihydro-pyrrol-2-one 2e.** MS (EI): *m/z* (%) 269 (M^+, 80), 240 ($C_{16}H_{18}NO^+$, 63), 226 ($C_{15}H_{16}NO^+$, 4), 187 ($C_{12}H_{13}NO^+$, 32), 172 ($C_{11}H_{10}NO^+$, 16) 158 ($C_{10}H_8NO^+$, 100), 144 ($C_{10}H_8O^+$, 10), 128 $C_{10}H_8^+$, 13), 115 ($C_9H_8^+$, 9), 103 ($C_8H_8^+$, 20), 91 ($C_7H_8^+$, 4), 77 ($C_6H_5^+$, 4), 55 ($C_4H_7^+$, 19), 41 ($C_3H_5^+$, 13); ^{1}H NMR ($CDCl_3$, 298 K) [ppm]: 0.87 (t, $^3J_{HH}$=7.8 Hz, 3H, CH_3), 1.04–1.81 (m, 10H, CH_2), 1.94–2.09 (m, 2H, CH_2), 3.85–4.01 (m, 1H, CH), 5.58 (d, $^3J_{HH}$=5.1 Hz, 1H,=CH), 6.62 (d, $^3J_{HH}$=5.1 Hz, 1H, =CH), 7.15–7.47 (m, 5H, $C_{ar}H$); ^{13}C NMR ($CDCl_3$, 298 K) [ppm]: 8.9 (CH_3), 25.2 (CH_2), 25.3 (CH_2), 25.4 (CH_2), 31.0 (CH_2), 31.6 (CH_2), 32.0 (CH_2), 50.3 (CH), 58.6 (C), 113.2 (=CH). 126.5 (=CH), 126.7 ($C_{ar}H$), 128.2 ($C_{ar}H$), 128.4 ($C_{ar}H$), 140.1 (C_{ar}), 178.9 (C=O); IR (GC-IR) [cm^{-1}]: 3069 w, 2973 w, 2943 vs, 2866 m, 1721 vs, 1604 w, 1495 w, 1454 w, 1376 m, 1324 w, 1297 w, 1266 m, 1248 m, 1201 w, 1137 w, 1032 w, 890 w, 802 w, 692 m.

***N*-cyclohexyl-3-ethyl-3-methyl-1,3-dihydro-pyrrol-2-one 2f.** MS (EI): *m/z* (%) 207 (M^+, 71), 192 ($C_{12}H_{19}NO^+$, 7), 178 ($C_{11}H_{17}NO^+$, 100), 164 ($C_{10}H_{15}NO^+$, 8), 150 ($C_9H_{13}NO^+$, 4),

136 ($C_8H_{11}NO^+$, 6), 125 ($C_8H_{13}O^+$, 13), 110 ($C_7H_{10}O^+$, 13), 96 ($C_7H_{12}^+$, 68), 81 ($C_6H_9^+$, 8), 67 ($C_5H_7^+$, 7), 55 ($C_4H_9^+$, 15), 41 ($C_3H_5^+$, 16); ^{1}H NMR ($CDCl_3$, 298 K) [ppm]: 0.69 (t, $^3J_{HH}$=7.4 Hz, 3H, CH_3), 1.12 (s, 3H, CH_3), 1.32–1.77 (12H, CH_2), 3.86–3.92 (m, 1H, CH), 5.20 (d, $^3J_{HH}$= 5.0 Hz, 1H,=CH), 6.46 (d, $^3J_{HH}$=5.0 Hz, 1H,=CH); ^{13}C NMR ($CDCl_3$, 298 K) [ppm]: 8.9 (CH_3), 22.0 (CH_3), 25.3 (CH_2), 25.4 (CH_2), 25.5 (CH_2), 30.0 (CH_2), 31.8 (CH_2), 32.2 (CH_2), 50.0 (CH), 51.3 (C), 115.1 (=CH), 127.3 (=CH), 181.6 (C=O); IR (KBr) [cm^{-1}]: 3354 w, 3090 s, 2963 vs, 2931 vs, 2855 vs, 1679 vs, 1602, 1450 s, 1402 s, 1385 s, 1359 m, 1344 s, 1327 m, 1311 s, 1261 vs, 1203 vs, 1140 s, 1050 w, 1029 w, 1007 m, 970 m, 933 w, 894 m, 806 w, 791 w, 757 m, 721 s, 693 vs, 627 w, 589 w, 547 w; CHN-analysis for $C_{13}H_{21}NO$: found (calcd) C 75.20 (75.31), H 10.25 (10.21), N 6.85 (6.76).

***N*-phenyl-9b-ethyl-4-propionyl-2,9b-dihydro-benzo[*e*]isoindol-1-one 5a.** MS (CI, H_2O): *m/z* (%) 344 (M^++H, 100); 314 ($C_{21}H_{16}NO_2^+$, 70); ^{1}H NMR ($CDCl_3$, 298 K) [ppm]: 0,84 (t, 3H, $^3J_{HH}$ =7.4 Hz, CH_3CH_2); 1.24 (t, 3H, $^3J_{HH}$=7.3 Hz, CH_3CH_2); 1.64–1.93 (m, 2H, CH_3CH_2); 2.87 (q, 2H, $^3J_{HH}$=7.3 Hz, CH_3CH_2); 7.17–7.50 (m, 10H, CH, Ar and CH 5-membered ring); 8.17 (d, 1H, $^3J_{HH}$=7.4 Hz, Ar); ^{13}C NMR ($CDCl_3$, 298K) [ppm]: 7.9 (CH_3CH_2); 8.4 (CH_3CH_2); 31.0 (CH_3CH_2); 37.1 (CH_3CH_2); 55.3 (C); 115.0 (=CH); 117.9 (=C); 122.1 (=CH); 125.2 (=CH); 126.0 (=CH); 127.2 (=CH); 128.2 (=CH); 129.1 (=CH); 129.2 (=CH); 129.5 (=C); 129.7 (=CH); 129.9 (=CH); 131.9 (=C); 133.6 (=CH); 136.6 (=C); 138.3 (=C); 177.0 (C=O); 199.8 (C=O); CHN-analysis for $C_{23}H_{21}NO_2$: found (calcd) C 79.98 (80.44), H 6.30 (6.16), N 4.03 (4.08); mp: 120°C.

***N*-cyclohexyl-9b-ethyl-4-propionyl-2,9b-dihydro-benzo-[*e*]isoindol-1-one 5b.** MS (CI, H_2O): *m/z* (%) 350 (M^+ +H, 100); 320 ($C_{21}H_{22}NO_2^+$, 20); 238 ($C_{17}H_{20}N^+$, 7); ^{1}H NMR ($CDCl_3$, 298 K) [ppm]: 0.69 (t, 3H, $^3J_{HH}$=7.4 Hz, CH_3CH_2); 1.13–1.16 (m, 1H, Cy); 1.18 (t, 3H, $^3J_{HH}$=7.3 Hz, CH_3CH_2); 1.32–1.45 (m, 4H, Cy); 1.63–1.85 (m, 7H, Cy and CH_3CH_2); 2.88 (q, 2H, $^3J_{HH}$=7.3 Hz, CH_3CH_2); 3.93–3.99 (m, 1H, Cy); 7,11 (s, 1H,=CH); 7.16 (s, 1H,=CH); 7.21–7.30 (m, 3H,=CH); 8.14 (d, 1H, $^3J_{HH}$=7.6 Hz, =CH); ^{13}C NMR ($CDCl_3$, 298 K) [ppm]: 7.7 (CH_3CH_2); 8.3 (CH_3CH_2); 25.2 (CH_2); 25.4 (CH_2); 25.5 (CH_2); 30.9 (CH_2); 31.7 (CH_2); 32.3 (CH_2); 36.7 (CH_2); 50.4 (CH); 54.9 (C); 116.5 (=C); 125.1 (=CH); 126.9 (=CH); 127.6 (=CH); 129.4 (=CH); 129.6 (=CH); 129.7 (=C); 132.0 (=C); 132.6 (=CH); 138.7 (=C); 177.8 (C=O); 200.1 (C=O); CHN-analysis for $C_{23}H_{27}NO_2$: found (calcd) C 77.82 (79.05), H 7.95 (7.79), N 3.95 (4.01); mp 171°C.

***N*-phenyl-3-propionyl-naphthyl-2-carbaldimine 6a.** MS (EI): *m/z* (%) 287 (M^+, 20), 230 ($C_{17}H_{12}N^+$, 11), 168 ($C_{12}H_8O^+$, 100), 153 ($C_{11}H_7N^+$, 11); ^{1}H NMR ($CDCl_3$, 298 K) [ppm]: 1.29 (t, 3H, J_{HH}=7.2 Hz), 3.05 (q, 2H, J_{HH}=7.2 Hz), the aromatic protons cannot be separated from the signals of **5a**.

***N*-cyclohexyl-3-propionyl-naphthyl-2-carbaldimine 6b.** MS (EI): *m/z* (%) 292 (M^+ -H, 16), 264 ($C_{18}H_{18}NO^+$, 24), 238 ($C_{17}H_{20}N^+$, 100), 208 ($C_{15}H_{14}N^+$, 24), 180 ($C_{13}H_{10}N^+$, 50), 168 ($C_{12}H_8O^+$, 16), 154 ($C_{11}H_8N^+$, 43), 140 ($C_{10}H_6N^+$, 21), 127 ($C_9H_5N^+$, 23); ^{1}H NMR ($CDCl_3$, 298 K) [ppm]: 1.34 (t, 3H, J_{HH}=7.3 Hz), 3.09 (q, 2H, J_{HH}= 7.3 Hz), the other cyclohexyl and naphthalene protons cannot be separated from the signals of **5b**.

Acknowledgements

The authors gratefully thank the *Deutsche Forschungsgemeinschaft* (SFB 436) for financial support.

References

1. (a) Brookhart, M.; Green, M. L. H. *J. Organomet. Chem.* **1983**, *250*, 395. (b) Constable, E. C. *Polyhedron* **1984**, *3*, 1037. (c) Halpern, J. *Inorg. Chim. Acta* **1985**, *100*, 41. (d) Crabtree, R. H. *Chem. Rev.* **1985**, *85*, 245. (e) Ryabov, A. D. *Chem. Rev.* **1990**, *90*, 403. (f) Davies, J. A., Ed.; *Selective Hydrocarbon Activation*, VCH: Weinheim, 1990. (g) Arndtsen, B. A.; Bergman, R. G.; Mobley, T. A.; Petersen, T. H. *Acc. Chem. Res.* **1995**, *28*, 154. (h) Crabtree, R. H. *Chem. Rev.* **1995**, *95*, 987. (i) Fujiwara, Y.; Takagi, K.; Taniguchi, Y. *Synlett* **1996**, 591. (j) Guari, Y.; Sabo-Etienne, S.; Chaudret, B. *Eur. J. Inorg. Chem.* **1999**, 1047. (k) Lavigne, G. *Eur. J. Inorg. Chem.* **1999**, 917. (l) Dyker, G. *Angew. Chem.* **1999**, *111*, 1808; *Angew. Chem. Int. Ed.* **1999**, *38*, 1698.

2. (a) Imhof, W. *J. Organomet. Chem.* **1997**, *533*, 31. (b) Imhof, W. *J. Organomet. Chem.* **1997**, *541*, 109. (c) Imhof, W.; Göbel, A.; Ohlmann, D.; Flemming, J.; Fritzsche, H. *J. Organomet. Chem.* **1999**, *584*, 33. (d) Imhof, W. *Organometallics* **1999**, *18*, 4845.

3. (a) Elsevier, C. J.; Mul, W. P.; Vrieze, K. *Inorg. Chim. Acta*, **1992**, 198–200, 689 and literature cited therein. (b) Mul; W. P.; Elsevier; C. J.; Polm; L. H.; Vrieze, K.; Zoutberg, M. C.; Heijdenrijk, D.; Stam, C. H. *Organometallics* **1991**, *10*, 2247. (c) Imhof, W. *J. Chem. Soc. Dalton Trans.* **1996**, 1429.

4. Imhof, W.; Göbel, A.; Braga, D.; De Leonardis, P.; Tedesco, E. *Organometallics*, **1999**, *18*, 736 and literature cited therein.

5. (a) Kakiuchi, F.; Yamauchi, F.; Chatani, N.; Murai, S. *Chem. Lett.* **1996**, 111. (b) Fukuyama, T.; Chatani, N.; Kakiuchi, F.; Murai, S. *J. Org. Chem.* **1997**, *62*, 5647. (c) Sonoda, M.; Kakiuchi, F.; Chatani, N.; Murai, S. *Bull. Chem. Soc. Jpn.* **1997**, *70*, 3117. (d) Fukuyama, T.; Chatani, N.; Tatsumi, J.; Kakiuchi, F.; Murai, S. S. *J. Am. Chem. Soc.* **1998**, *120*, 11522.

6. Berger, D.; Imhof, W. *J. Chem. Soc., Chem. Commun.* **1999**, 1457.

7. Morimoto, T.; Chatani, N.; Murai, S. *J. Am. Chem. Soc.* **1999**, *121*, 1758.

8. (a) Laine, R. M. *J. Mol. Catal.* **1982**, *14*, 137. (b) Hilal, H. S.; Jondi, W.; Khalaf, S.; Abu-Halawa, R. *J. Organomet. Chem.* **1993**, *452*, 161. (c) Hilal, H. S.; Khalaf, S.; Jondi, W. *J. Organomet. Chem.* **1993**, *452*, 167. (d) Adams, R. D.; Barnard, T. S.; Li, Z.; Wu, W. *J. Am. Chem. Soc.* **1994**, *116*, 9103.

9. Crystal data for $C_{13}H_{21}NO$ **2f**: M=207.31, orthorhombic, a=20.476(1), b=22.094(1), c=11.4430(4) Å, V=5176.8(5) Å^3, space group *Fdd*2, Z=16, 1376 reflections measured, 1376 unique, 1253 observed reflections ($F_o^2>2\sigma(F_o^2)$), $R1$=0.0562, $wR2$= 0.1395, *GooF*=1.081, largest diff. peak 0.129 e Å^{-}3.

10. *Crystal data* for $C_{23}H_{27}NO_2$ **5a**: M=343.41, monoclinic, a=11.1284(5) Å, b=17.7043(6) Å, c=18.5853(8) Å, β=97.17(2)°, V=3633.1(3) Å3, space group C2/*c*, Z=8, 13 588 reflections measured, 4089 unique (R_{int}=0.0483), 3248 observed reflections ($F_o^2>2\sigma(F_o^2)$), R_1=0.0632, wR_2=0.1263, *Goof*=1.117, largest diff.

peak and hole 0.214 and −0.145 e Å^{-3}. *Crystal data* for $C_{23}H_{27}NO_2$ **5b**: M=349.46, orthorhombic, a=16.9615(4) Å, b=11.3614(3) Å, c=19.9566(6) Å, V=3845.8(2) Å^3, space group $Pna2_1$, Z=8, 8449 reflections measured, 8449 unique, 5504 observed reflections ($F_o^2>2\sigma(F_o^2)$), R_1=0.0774, wR_2=0.1527, *Goof*=1.037, largest diff. peak and hole 0.322 and −0.249 e Å^{-3}.

11. (a) Gamzu, E. R.; Hoover, T. M.; Gracon, S. I. *Drug. Dev. Rev.* **1989**, *18*, 177. (b) Bertozzi, S.; Salvadori, P. *Synth. Commun.* **1996**, *26*, 2659.
12. (a) Sheldrick, G. SHELXS-86, Universität Göttingen, 1986. (b) Sheldrick, G. SHELXL-93, Universität Göttingen, 1993.
13. Zsolnai, L.; Huttner, G. XPMA, Universität Heidelberg, 1996.
14. Siemens Analytical X-ray Inst. Inc., XP-Interactive Molecular Graphics, Vers. 4.2, 1990.